Appl. Phys. B 90, 329–337 (2008)
DOI: 10.1007/s00340-007-2926-x

Applied Physics B
Lasers and Optics

K.G. HAY
S. WRIGHT
G. DUXBURY✉
N. LANGFORD

In-flight measurements of ambient methane, nitrous oxide and water using a quantum cascade laser based spectrometer

Scottish University Physics Alliance, Department of Physics, John Anderson Building, University of Strathclyde, 107 Rottenrow East, Glasgow G4 0NG, UK

Received: 15 September 2007 /
Revised version: 20 November 2007
Published online: 22 January 2008 •

ABSTRACT In-flight measurements of ambient methane, nitrous oxide and water have been made using frequency down-chirped radiation from a compact, pulsed, quantum-cascade laser spectrometer. In three flights from Oxford airport in October 2006 the variations of the concentration of these three trace gases could be measured and related to possible sources in the flight path.

PACS 33.20.EA; 42.62.Fi; 42.68.Ca; 85.35.Be

1 Introduction

Methane and nitrous oxide are two of the main gases monitored as part of a worldwide measurement programme for greenhouse gases [1, 2]. The main organisation which reviews the contribution of greenhouse gases to global warming is the Intergovernmental Panel on Climate Change (IPCC) [2]. The current average tropospheric concentrations of methane and nitrous oxide in February 2005 have been given by Blasing and Jones [1], who have summarised the results from the Carbon Dioxide Information Analysis Center (CDIAC) project [1]. Measurements are usually referred to the background levels in clean sites with little exposure to industrial pollution. The closest reference site of this kind for the UK is Mace Head on the west coast of Ireland. The background concentrations of nitrous oxide and methane used in this paper are taken from the 2005 Mace Head values [1].

We have developed a compact intra-pulse approach QC laser spectrometer [3] which is suitable for measuring the concentrations of ambient levels of methane and in an earlier flight from Oxford airport demonstrated its potential for making atmospheric measurement of methane and nitrous oxide. We have since greatly increased the path length, installed a wider bandwidth detector, and improved the electrical isolation of the instrument [4]. This improved system was flown on three flights from Oxford airport in October 2006. The results obtained from these flights are used to demonstrate this improved spectrometer is well suited to in-flight measurements of the variability of trace gas concentrations.

✉ Fax: +44-141-552-2891, E-mail: g.duxbury@strath.ac.uk

2 Spectrometer arrangement and performance

The basic design of this spectrometer is identical to that used in the previous flight test [3]. One of the main changes which we have made is to increase the separation of the astigmatic Herriot cell mirrors to 50 cm, and to alter the initial input direction of the laser beam. This has allowed us to increase the path length from 27.7 to 99.6 m. We have also used a wider bandwidth infrared detector, which did not require a reverse bias voltage, and eliminated the electrical interference problems encountered previously. A photograph of the optical breadboard is shown in Fig. 1a.

The spectrometer is controlled by a LabVIEW 7.1 virtual instrument (VI), running on a PC. The control cards, including the digitiser are housed in PCI slots in this computer. Once the initialization has been carried out, the program runs continuously. Background spectra of zero grade air are taken at the desired interval. The instrument can therefore run unattended, and was used in this mode of operation in a series of recent experiments at the NERC CEH laboratory at Penicuik in July 2007 [4, 5].

A schematic of the vacuum system is shown in Fig. 1b. A constant flow through the cell is created by the pump. The pump used in the plane is an oil-free pump with flow rate of 6 m^3/h and a 150 mbar vacuum capability, permitting a 2 s gas exchange time for the absorption cell. The atmosphere is sampled through a forward facing sampling inlet at the front of the aircraft [6], shown in Fig. 2. The incoming air either passes through the mass flow controller, or is diverted into the cabin while background spectra are recorded. The mass flow controller is set to try to maintain a constant pressure of 100 Torr within the cell for both background and atmospheric samples. To record a background spectrum, the in-flow is diverted to the cabin, and the cell is evacuated for 30 s. Another valve is then opened to a cylinder of zero grade air. There is a 60 s delay to allow the zero air to flush out any remaining gases, then the background spectrum is recorded. The valve to the atmosphere is then reopened, and following a 40 s flushing delay, the spectral recording is resumed.

a

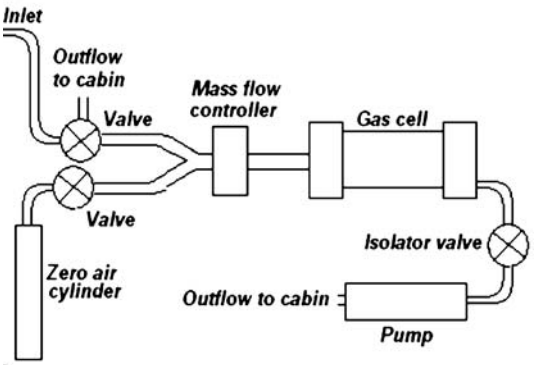

b

FIGURE 1 (**a**) The optical breadboard, MCT detector bottom left hand side (LHS), laser head centre LHS, laser power supply, top LHS. Absorption cell, right hand side. (**b**) Schematic of the vacuum system

The QC laser was operated in pulsed mode, a 1300 ns top-hat shaped current pulse was applied to the distributed feedback (DFB) QC laser operating at 7.84 μm. The resultant rapid frequency down-chirp is used to scan through the absorption spectrum, giving a frequency scan range of ca. 97.5 GHz. The length and relative tuning rate of the laser is measured using the fringe pattern recorded on a spectrum when the movable germanium etalon is introduced into the beam path. This etalon fringe pattern is recorded at the start of each spectral recording session.

The laser beam leaving the gas cell is focussed onto an HgCdTe (MCT) photovoltaic detector with a bandwidth of ca. 400 MHz. The signal produced from this is then amplified by a 2 GHz bandwidth amplifier, which is connected to a 2 Gs Aquiris digitiser and averager, with step width of 0.5 ns. The averaged spectra are then transferred to the main data storage area on the acquisition computer. They are subsequently processed on a laboratory based computer using a new analysis programme based on LabVIEW 8.0 VI's .

To ensure that the spectral output covered several methane, nitrous oxide and water absorption lines during one

FIGURE 2 The forward facing inlet, mounted on the aircraft roof, is used to sample the atmosphere

pulse the substrate temperature of the QC laser was set to 2 °C. The pulse duration was 1.3 μs, the pulse repetition frequency 20 kHz, and the operating voltage 11.5 V. 20 000 successive spectra were averaged. The software determined time interval between successive recorded spectra is 2.8 s. As the frequency down-chirp rate of the first part of the frequency-swept pulse is very rapid, only the spectra recorded using the slower chirp in the second part of the pulse have been used in the present study.

The flight path and altitude were recorded as RINEX files using the GPS data logging system within the aircraft. This was then post-processed using the P4 software, which forms part of the GRINGO package produced by the Institute of Engineering Surveying and Space Geodesy at Nottingham University, and the plotted using ArcMap v9.1 from the ESRI ArcGIS 9 software suite. After a comparison of the time stamp of the GPS system and that of the control computer, it was discovered that the computer clock was 3 min slow. A time cor-

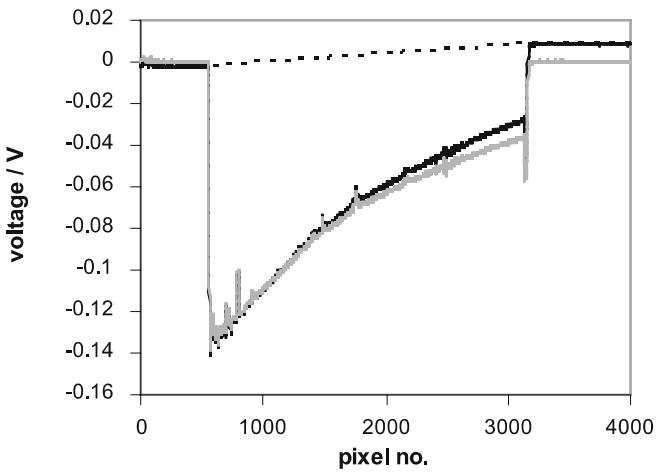

FIGURE 3 Raw spectrum (*black*), baseline correction factor (*dashed*), and corrected spectrum (*grey*)

rection has therefore been made to allow the spectra recorded during the flights to be reconciled with the GPS data.

3 Analysis

On the first flight, it became apparent that the valve connecting the manifold to the zero air cylinder was malfunctioning, with the result that the "background" spectra were recorded with residual atmospheric gases within the absorption cell. In order to overcome this problem the background spectra were derived from the recorded spectra by a self-calibration approach. All of the data analysis described in this paper was carried out using our group's own LabVIEW virtual instruments, written specifically for the purpose.

As a result of the ac coupling between the photodiode amplifier and the digitiser, all spectra required a correction to the baseline, shown in Fig. 3. The mean baseline value before and after the pulse is subtracted, and a linear baseline correction is calculated and subtracted across the pulse. The effects of this correction are shown in Fig. 3.

Much of the repetitive noise in the spectra is a consequence of the digitisation process carried out by the Aquiris card. In order to derive an accurate background spectrum, this artefact must be removed. The periodic digitiser noise is then added to the background spectrum, in order to achieve cancellation of the effects of this artefact during calculation of the transmission spectrum. This is similar to the cancellation of noise in the method of Nelson et al. [7]. To accomplish this, each spectrum was smoothed by a 9-point Savitzky–Golay smoothing algorithm [8]. The ratio of the original signal to the smoothed signal was taken to give a roughening, or noise function corresponding to the periodic digitiser noise. The background was then obtained from the smoothed spectrum by approximating the segment of baseline across each absorption line by linear interpolation. The derived background spectrum was then re-roughened to give a background con-

			CH_4			
Wavenumber [a] [cm^{-1}]	Vibrational transition	J'_m	$J''_{m''}$	S, integrated intensity[b]	γ_{air} [cm^{-1}/atm]	label
1276.84431	4^1_0, ^{12}C	$4F_1$	$5F_{2'}1$	3.73	0.065	m1
1275.38678	4^1_0, ^{12}C	$4E$	$5E$	2.46	0.055	m2
1275.04168	4^1_0, ^{12}C	$4F_2$	$5F_{1'}2$	3.69	0.061	m3
			N_2O			
Wavenumber [a] [cm^{-1}]	Vibrational transition	J'	J''	S, integrated intensity[b]	γ_{air} [cm^{-1}/atm]	label
1276.36576	3^1_0	9	10	13.56	0.0827	n1
1275.49287	3^1_0	10	11	14.23	0.0817	n2
1274.61651	3^1_0	11	12	14.76	0.0807	n3
			H_2O			
Wavenumber [a] [cm^{-1}]	Vibrational transition	$J'_{K_{a'}K_{c'}}$	$J''_{K_{a''}K_{c''}}$	S, integrated intensity[b]	γ_{air} [cm^{-1}/atm]	label
1276.62804	2^1_0	$15_{1,15}$	$16_{0,16}$	1.82×10^{-4}	0.0064	w1
1276.62619	2^1_0	$15_{0,15}$	$16_{1,16}$	5.45×10^{-4}	0.0065	w1
1275.66245	2^1_0	$8_{3,5}$	$9_{3,6}$	1.38×10^{-4}	0.0851	w2

[a] Ref. [8]
[b] Intensities in 10^{-20} cm/molecule

TABLE 1 Assignment, intensities and air broadening parameters of observed CH_4, N_2O and H_2O absorption lines. The pressure broadened widths are half width at half maximum (HWHM)

Molecule[a]	Wavenumber[a]	Obs. FWHM[b]	Calc. FWHM, Doppler	Calc. FWHM[c], chirp rate	Calc. FWHM[a], air broadening
H_2O, w2	1275.66245	0.024	0.0037	0.0068	0.0215
CH_4, m2	1275.38678	0.018	0.0040	0.0064	0.0140
CH_4, m3	1275.04168	0.018	0.0040	0.0059	0.0154
N_2O, n2	1275.49287	0.024	0.0024	0.0067	0.0206
N_2O, n3	1274.61651	0.021	0.0024	0.0052	0.0204

[a] see Table 1
[b] measured using the spectra shown in Fig. 4
[c] assuming a Gaussian instrument function, see [10]

TABLE 2 Contribution to the full width at half maximum height, (FWHM) [cm^{-1}], of the absorption lines at a reduced atmospheric pressure of 96 Torr

taining the periodic digitiser noise. The transmission spectrum is then calculated by taking the signal to background ratio. This is divided by its own mean value to adjust the baseline to 1. Finally, the spectra are converted from pixel number to wavenumber/cm^{-1}, using the etalon fringe spacing to give a relative wavenumber tuning, with the wavenumber/cm^{-1} of the absorption lines themselves used to provide an absolute calibration. The wavenumbers of the absorption lines are given in Table 1.

A peakfitting program developed for this project is based upon numerical functions provided in Labview. This program is used to remove any remaining slope in the baseline and fit a Lorentzian function to each peak. Although the Voigt function is a more accurate description of the line shape, at the gas pressure used for the experiments the dominant source of line broadening is due to collisions of the trace gas molecules of water, methane and nitrous oxide with the background of nitrogen and oxygen, leading to a predominantly Lorentzian shape. The other source of broadening is instrumental and is due to the rapid laser down-chirp, and is proportional to the square root of the chirp rate [10]. The calculated contributions of the Doppler effect, foreign gas broadening and instrumental broadening are given in Table 2.

In the peakfitting program, the parameters used to fit the lineshape are used to calculate the integrated intensity of the peak, and thus the concentration of gas. The program output consists of a list of date-stamps and concentrations calculated from each spectral line.

The average amount of nitrous oxide in the atmospheric background at mid-latitudes in the northern hemisphere is 319 parts per billion by volume (ppbv), whereas that of methane is much greater, 1852 ppbv [1]. However, the absorption cross section of the absorption lines of the 8 μm ν_3 vibration rotation band of nitrous oxide is much larger than those of the ν_4 band of methane, see Table 1, so that the absorbance of the absorption lines of these gases in our spectral region are similar. The close proximity of the methane and nitrous oxide absorption lines allows simultaneous monitoring, as noted by Webster et al. [11] and Nelson et al. [7], and hence accurate measurement of their relative concentration ratio.

Typical spectra recorded during the take-off at Oxford airport, and in the final approach to the descent to the landing at Haverfordwest airport, are shown in Fig. 4a and b. The difference in methane mixing-ratio is very clear, while the nitrous oxide concentration hardly changes. The variation in water mixing-ratio can also be examined, as shown in Fig. 4c. During the descent, there is a significant increase in absorbance of the infrared vibration–rotation line of water, and hence of the concentration. However, in these spectra only minor changes in the methane and nitrous oxide concentrations are observed. The signal to noise ratio in these spectra is similar to that obtained by Webster et al. [11] in the flight spectra of nitrous oxide and methane recorded at up to 20 km using the NASA ER-2 aircraft. The second derivative spectra were measured using a cw QC laser scanning from 1256.8 to 1256.2 cm^{-1} and a path length of 80 m in the 1 m long Herriott cell of the ALIAS underwing instrument. The quality of the spectra is also similar to those of nitrous oxide and methane recorded by Nelson et al. [7] at ambient concentration in laboratory room air, using the inter-pulse Aerodyne QC spectrometer. Its

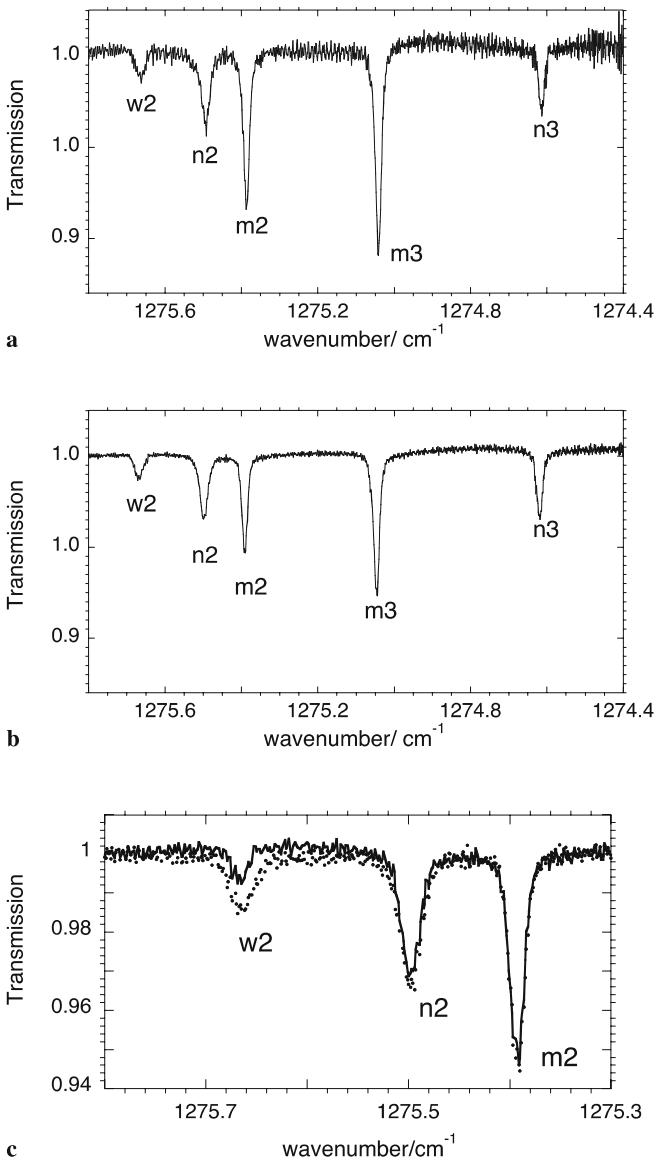

FIGURE 4 Samples in of flight spectra: (**a**) takeoff from Oxford airport, (**b**) descending to Haverfordwest airport. (**c**) A comparison of the intensity of the water absorption line, w2, at mid flight (*black*), and on landing at Haverfordwest (*grey*)

multipass absorption cell was an astigmatic Herriott cell with optical path length of 56 m, and operated with a pressure of either 50 or 60 Torr within the cell.

4 Results

The outward and return flight paths between Oxford and Haverfordwest airports are shown in Fig. 5. The original intention had been to fly the same route in both directions, but at differing altitudes, but this was impossible owing to air traffic control restrictions. On the outward flight the plane flew at an altitude of about 600 m, whereas the altitude of most of the return flight was much greater, about 2000 m. The altitudes for both the outbound and return flights, logged by the GPS system in the plane, using Greenwich Mean Time (GMT), are shown in Fig. 6a and b. The variation of the pressure within the absorption cell during the flights

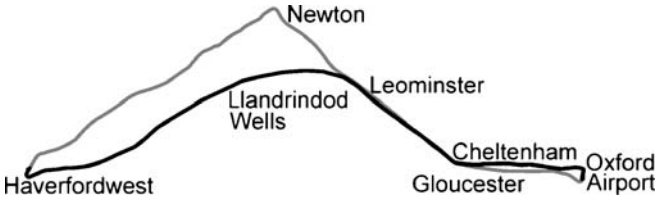

FIGURE 5 Flight path from Oxford to Haverfordwest (*grey*) and return flight (*black*), derived from the GPS map

is also plotted, using the computer time system, British summer time (BST). The latter plot is adjusted owing to the error in the computer clock referred to earlier. It may be noted that the pressure fluctuations observed during the flight are much larger in the outbound low altitude leg, where the flight conditions were quite turbulent. The long-term pressure variation measured during the flight is reversed in the return leg, and is probably due to the variation in atmospheric pressure between Oxford airport and that at Haverfordwest. In a subsequent

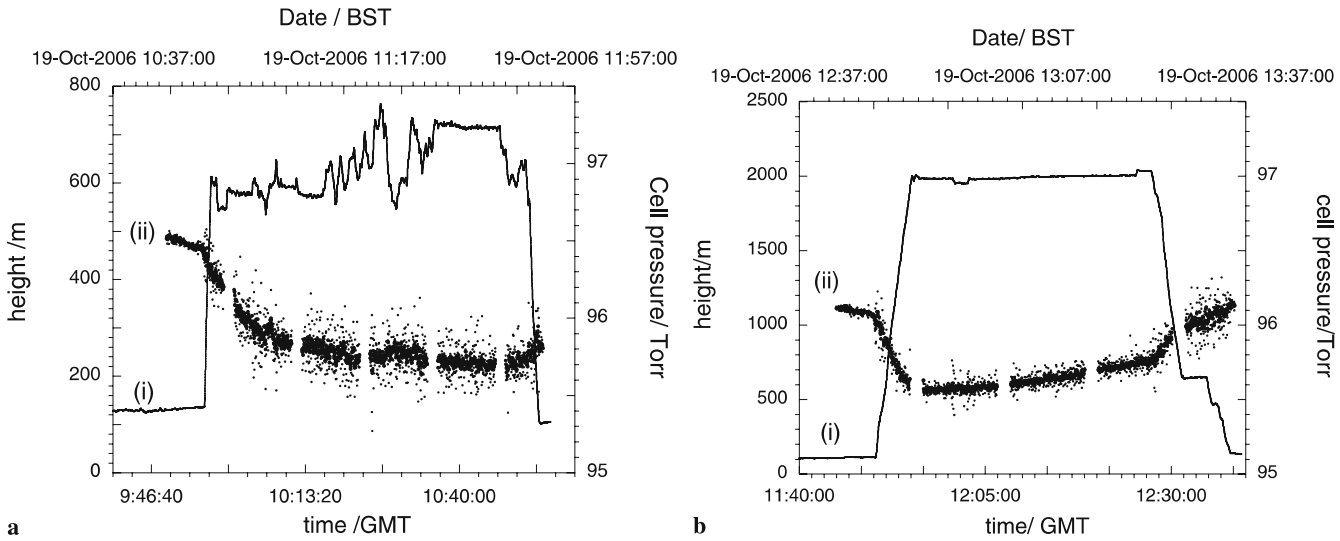

FIGURE 6 Flight altitude, and pressure variation within the absorption cell, from Oxford to Haverfordwest, low level (**a**); and return flight, higher level (**b**). In the plotted pressure variation the *filled circles* correspond to using a five point data smoothing, which helps to pick out the correlation between the rapid altitude changes and abrupt fluctuations in cell pressure. Note that in both (**a**) and (**b**) the large fluctuations in cell pressure correspond to rapid changes in altitude

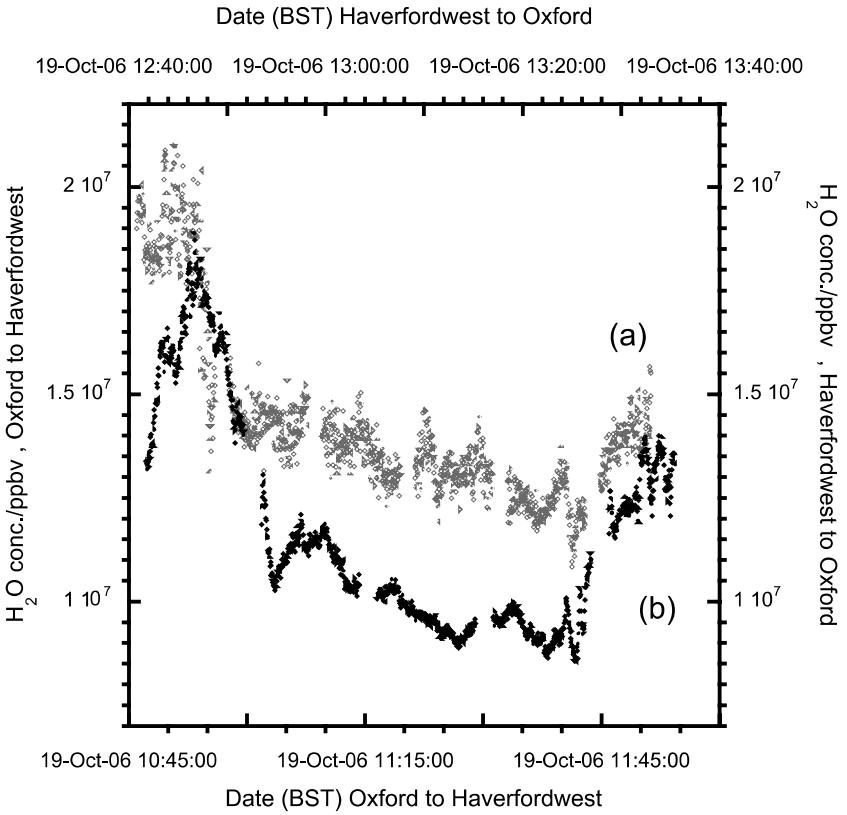

FIGURE 7 Water vapour concentrations measured on the flights between Oxford and Haverforwest airports. (a) Outbound flight, (b) return flight. Concentrations on outward flight. The mixing ratio for the saturation vapour pressure at 20 °C is 0.023 (2.3×10^7 ppmv) [12], so at the maximum concentrations measured the air was close to being saturated

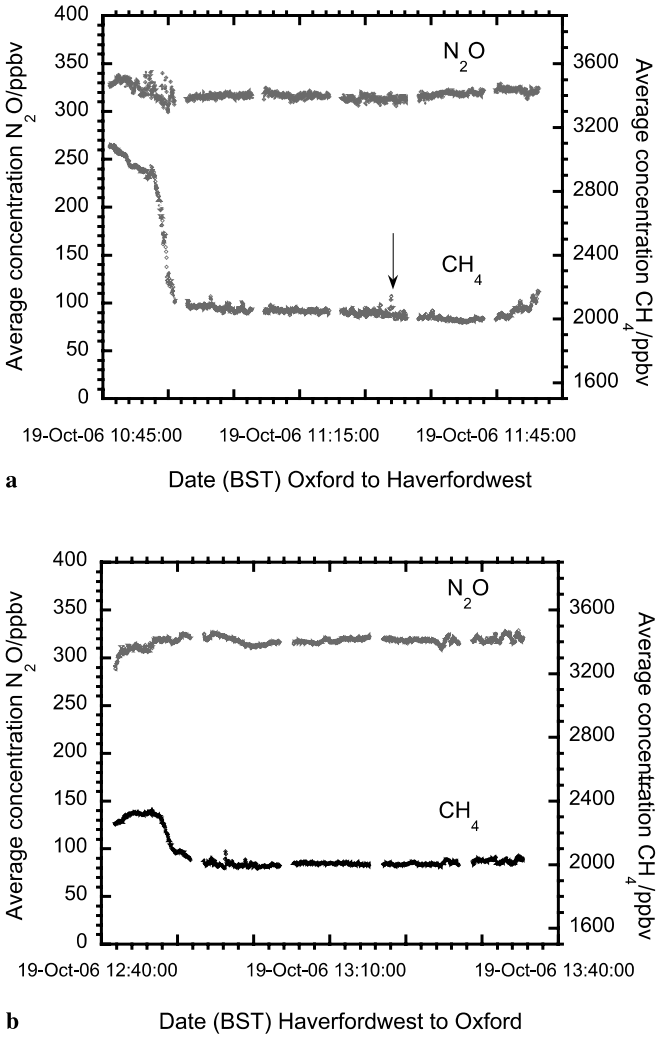

a

b

FIGURE 8 Methane and nitrous oxide concentrations measured on the flights between Oxford and Haverfordwest airports. (**a**) Outbound flight, (**b**) return flight. For comparison the northern hemisphere (NH) background levels for nitrous oxide are 319 ppbv and for methane are 1852 ppbv [1]. It may be seen that although the nitrous oxide concentrations measured are close to those of the NH background, those of methane are significantly larger. A rapid local increase in the methane concentration observed in the outbound flight is indicated by the *arrow*

closed loop flight from Oxford airport the long-term variation was absent. The average cell pressure of ca. 96 Torr was less than the 100 Torr set on the mass flow controller, and varied most on takeoff when the ram effect changed rapidly as the plane gathered speed. This pressure change is not as evident on landing as the spectrometer acquisition had to be switched off soon after touchdown, when the aircraft was still travelling at high speed.

The trace gas concentrations were derived from the experimental spectra using the method discussed in the previous Sect. 3. Figure 8 shows the concentrations of nitrous oxide and methane recorded during the flights between Oxford and Haverfordwest airports. The outbound flight concentrations are in Fig. 8a, and those from the return flight in Fig. 8b.

Figure 7 shows the derived water concentrations, (a) on the outbound flight (b) on the return flight. Figure 9 shows the $CH_4 : N_2O$ ratio for the two flights. This ratio may be used to demonstrate that the fluctuations in methane are not due to instrumental noise. If their origin were due to fluctuations in the gas pressure within the absorption cell, both the methane and the nitrous oxide would be affected similarly, and hence the rapid fluctuation of the amount of methane would not be apparent in the ratioed concentrations. The major in-flight fluctuation in the concentration of methane is indicated by the arrows in Figs. 8a and 9.

There are clear variations in trace gas mixing ratios during the flights, the most prominent feature being the rapid decrease in the concentrations in methane and water from their high initial levels. On takeoff from Oxford the methane level dropped from 3100 ppb to 2100 ppb of methane. Oxford airport is surrounded by busy roads, which give a high methane level. Additionally, during the instrument initialisation, the plane was stationary, creating a high local concentration of pollutants. The time delay between the start-up of the plane engines until the first spectrum was recorded was about 5 min, allowing a static region of polluted air to develop in the vicinity of the aircraft. This polluted air was sucked into the cell by the pump, leading to a very high concentration of methane and water in the absorption cell while the aircraft was stationary. As the taxi speed of the aircraft is slow, it is not until the aircraft reaches its cruising speed of ca. 310 km/h that the ram effect of the sampling inlet is maximised. As a result the time taken from the start of the spectrometer recording, until the trace gas concentrations approached their local background levels, was about 8 min.

In the concentration profile recorded in the flight from Oxford to Haverfordwest airport, there is clear evidence for a rapid increase in the concentration of methane, a localised spike, at 11:29 BST (10:26 GMT). This is indicated by the arrow in Fig. 8a. This corresponds to flying across a funnel shaped valley in range of hills near a junction on a major tourist route (see Fig. 10). The funnel effect resulted in the plane being pushed upwards, as shown in the flight altitude profile in Fig. 6, while creating a column of more strongly polluted air which we flew through. A possible source for this is traffic generated pollution from the major road at the foot of the hill.

The third flight was a circuit around Oxfordshire. A map of this flight is shown in Fig. 11, and the altitude and cell pressure variation in Fig. 12. The methane and nitrous oxide concentrations are shown in Fig. 13, the water vapour concentration in Fig. 14, and the methane to nitrous oxide ratio is shown in Fig. 15.

By comparing the ratios of methane to nitrous oxide shown in Figs. 9 and 15 it may be seen that much of the initial high level of methane must be due to the overall methane loading of the air at the particular airport location. The lower methane level recorded when taking off from Haverforwest, than from Oxford airport, may be correlated with a much greater number of aircraft and their movements at Oxford compared with those at Haverfordwest airport.

A comparison of the water concentrations measured in the three flights shows that the largest concentration of 2×10^7 ppbv (2%), is close to that of saturated air at 20 °C [12]. The large fluctuations in the concentration of water vapour in comparison with those of methane and nitrous oxide correlate well with the weather conditions over South Wales and the Oxford region on October 19th and 20th 2006.

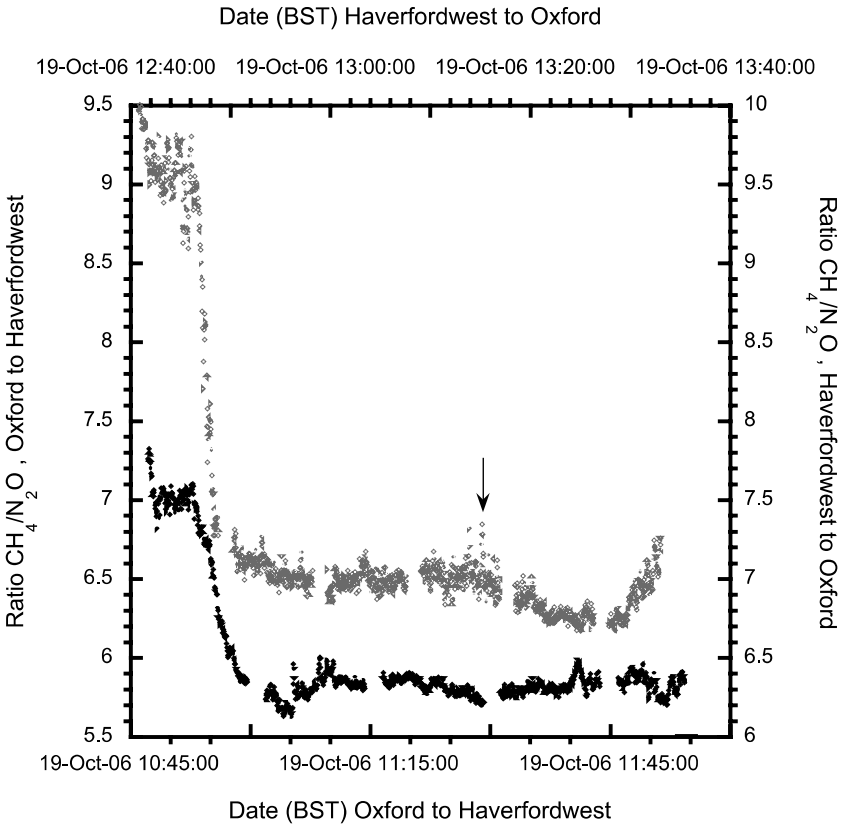

FIGURE 9 The ratio of the concentrations of methane to nitrous oxide measured on the flights between Oxford and Haverfordwest airports. (*Grey*): outbound flight, (*black*): return flight. This concentration ratio for the NH background levels is 5.8 [1]. The rapid change in the methane concentration noted in Fig. 8a is also seen here, showing that there is no corresponding rapid fluctuation in the concentration of nitrous oxide

The root mean square (rms) noise level for the concentration of methane over the period of the flights was 5 ppb, and for nitrous oxide 1 ppb. These compare well with those reported by Nelson et al. [7].

The reason why a comparatively large pressure of ca. 100 Torr is used in the absorption cell is to increase the number density and also the gas collision frequency. Although the greater number of collisions increases the pressure broadening, it also ensures that the collision frequency is fast in comparison with that of the rapidly swept laser. This eliminates rapid passage effects which can cause the absorption line shape to become quite asymmetric as described in detail by Duxbury et al. [13]. Under these higher pressure conditions the instrumental lineshape is a Gaussian function, whose full width at half maximum is determined by the square root of the chirp rate as described previously [10].

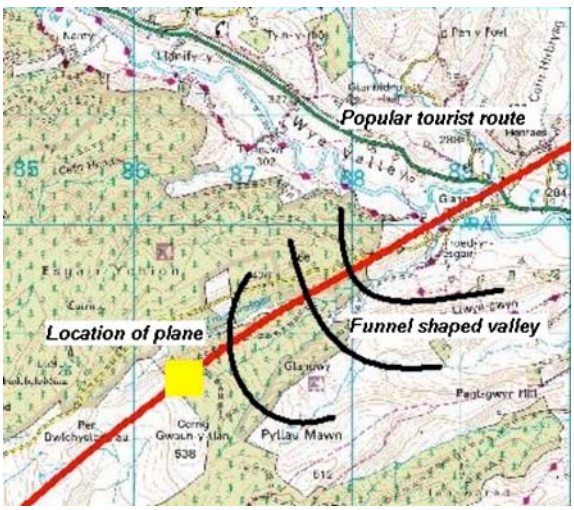

FIGURE 10 Location of aircraft while detecting the rapid increase in methane (a methane "spike"). © Crown Copyright/database right 2007. An Ordnance Survey/EDINA supplied service

5 Conclusions

Utilising the wide tuning range of the intra-pulse QC laser allows us to measure the ambient atmospheric concentrations of methane and nitrous oxide and water using pairs of absorption lines which are well resolved. The changes to the mirror spacing within the absorption cell have allowed us to obtain a greatly increased path length over that

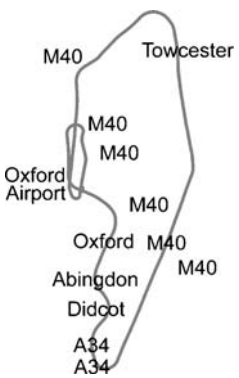

FIGURE 11 Flight path of the Oxfordshire circuit. The locations of the major trunk roads, the M40 and the A34, relative to the flight path are indicated

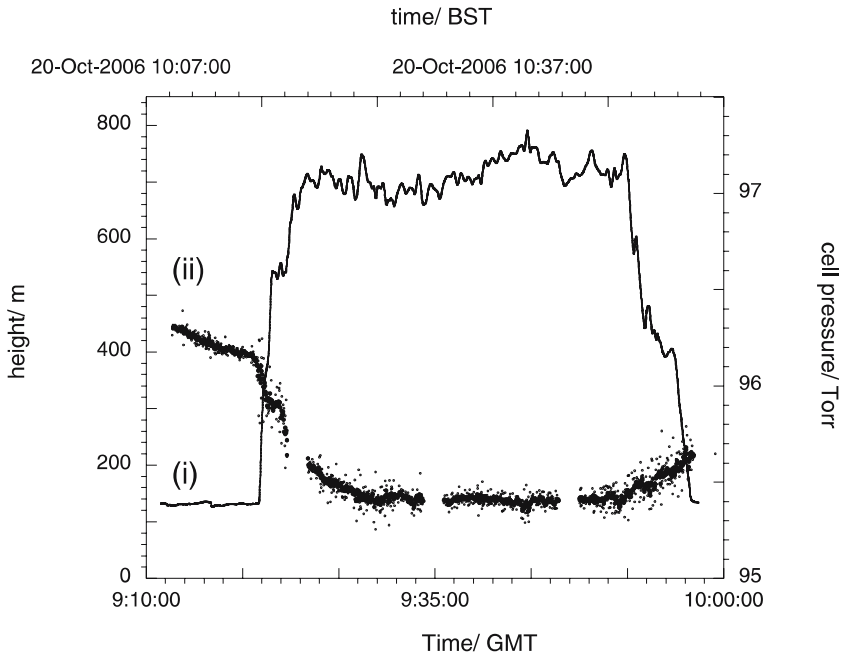

FIGURE 12 Altitude of the aircraft, and pressure within the absorption cell, during the Oxford circuit. For additional details see Fig. 6

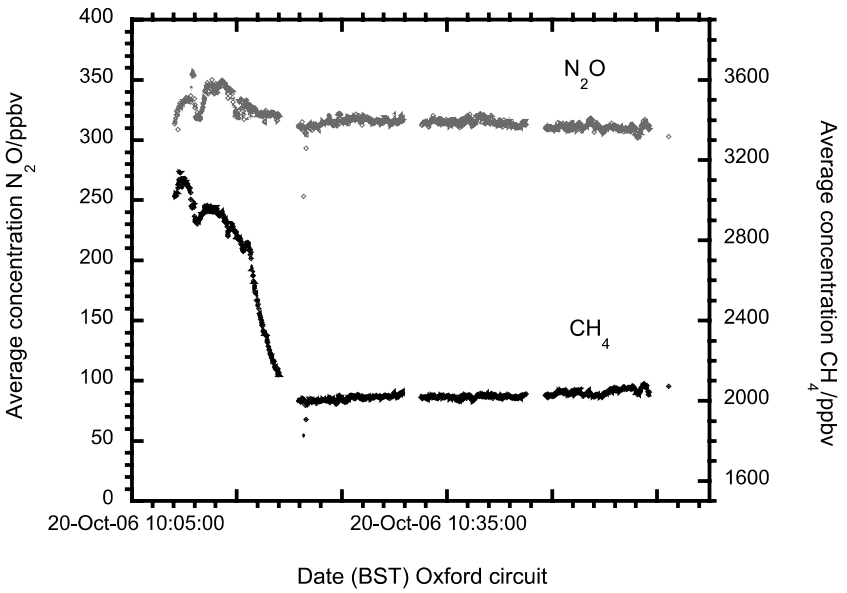

FIGURE 13 Methane and nitrous oxide concentration during the Oxford circuit, for comparison see Fig. 8

used previously [3]. This modification has increased the absorbance by a factor of three, which has allowed us to use the weak 1275.66 cm^{-1} absorption line of water to measure the water vapour concentration, rather than the Dicke narrowed line [14] at 1276.63 cm^{-1}. It is more difficult to use this very narrow line to derive the concentration of water vapour, since it occurs at the start of the frequency sweep, where the sweep rate is very rapid leading to a very asymmetric line shape [13], and where the laser power output has a very oscillatory structure.

The signal to noise ratio that we have obtained is close to that demonstrated in a laboratory environment [3], showing that the instrument is almost immune to the in-flight vibrations of the aircraft. We attribute that partly to the fact that in our intra-pulse spectrometer a single spectrum is recorded in ca. 1.3 μs, so that there is no vibrational noise contribution within the recording period.

ACKNOWLEDGEMENTS We are grateful to the EPSRC for the grant of a studentship through the Doctoral Training Fund. We are also indebted to the NERC for the award of the COSMAS grant which funded much of the instrument development, and to the NERC Airborne Research and Survey Facility (ARSF) for the research flight time granted for the use of their aircraft. We are also very grateful to Carl Joseph and David Davies of ARSF, Oxford for their help before and during the flight campaign.

REFERENCES

1 T.J. Blasing, S. Jones, Current Greenhouse Gas Concentrations, Carbon Dioxide Information Analysis Center (CDIAC), Oak Ridge National Laboratory, USA
2 IPCC 2001, *Climate Change 2001: The Scientific Basis* (Cambridge University Press, Cambridge, UK, 2002)
3 S. Wright, G. Duxbury, N. Langford, Appl. Phys. B **85**, 243 (2006)
4 G. Duxbury N. Langford, S. Wright, K. Hay, Development of the Strathclyde University QC laser spectrometer for the measurement of methane, nitrous oxide and water on the NERC ARSF Dornier Aircraft, presented at the 6th Int. Conf. on Tuneable Diode Laser Spectroscopy, Reims, France, July 2007

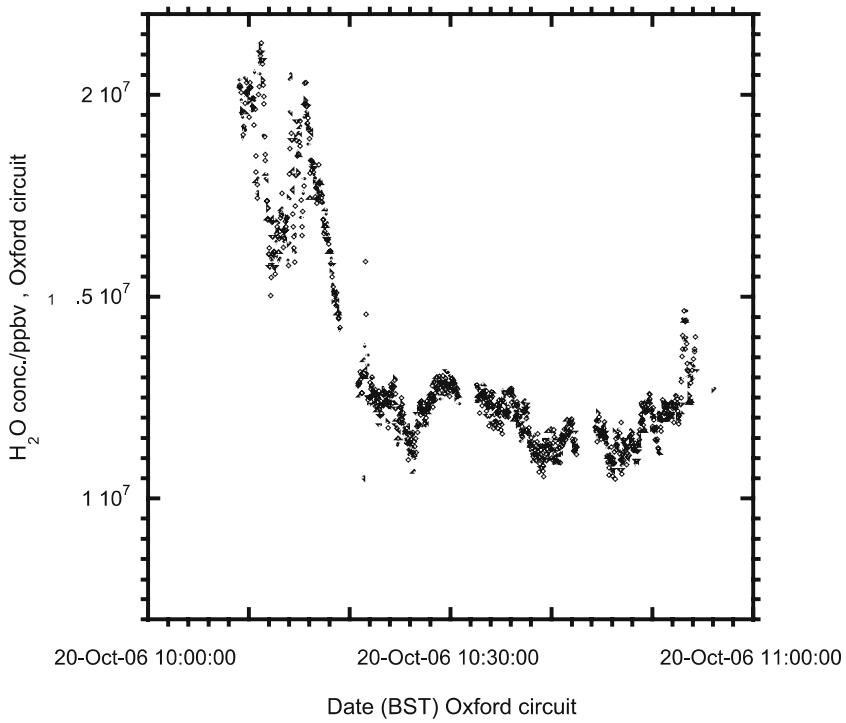

FIGURE 14 Water vapour concentration during the Oxford circuit, for comparison see Fig. 7

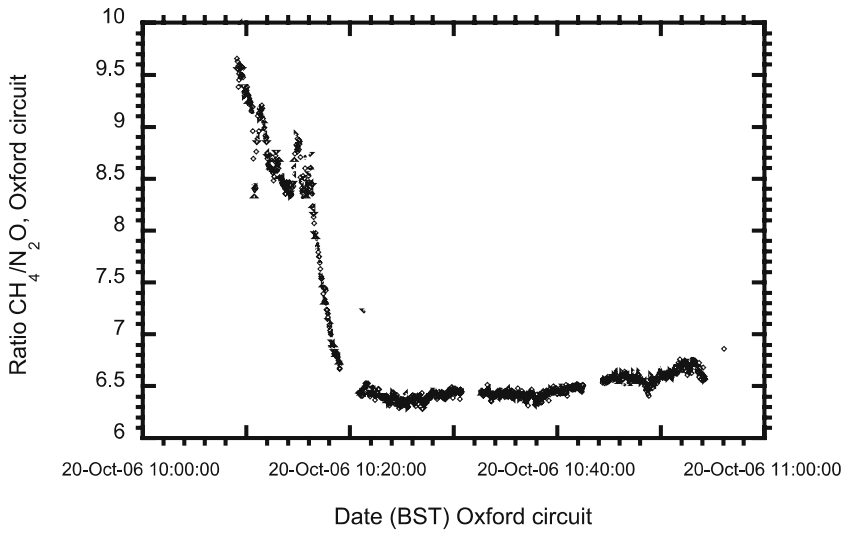

FIGURE 15 Methane to nitrous oxide ratio during the Oxford circuit, see Fig. 9 for comparison

5 K. Hay, G. Duxbury, N. Langford, Quantum Cascade Laser Spectrometer Measurements of Atmospheric Water, Nitrous Oxide and Methane Levels, presented at the 2nd Int. Workshop on Infrared Plasma Spectroscopy, Greifswald, Germany, July 2007
6 NERC Dornier 228 Aircraft, NERC ARSF, Hangar 2, Oxford Airport, Kidlington, Oxon OX5 1RA
7 D.D. Nelson, J.B. McManus, S. Urbanski, S. Herndon, M.S. Zahniser, Spectrochim. Acta A **60**, 3325 (2004)
8 A. Savitzky, M.J.E. Golay, Anal. Chem. **46**, 1627 (1964)
9 L.S. Rothman, A. Barbe, D.C. Benner, L.R. Brown, C. Camy-Peyret, M.R. Carleer, K. Chance, C. Clerbaux, V. Dana, V.M. Devi, A. Fayt, J.-M. Flaud, R.R. Gamache, A. Goldman, D. Jacquemart, K.W. Jucks, W.J. Lafferty, J.-Y. Mandin, S.T. Massie, V. Nemtchinov, D.A. Newnham, A. Perrin, C.P. Rinsland, J. Schroeder, K.M. Smith, M.A.H. Smith, K. Tang, R.A. Toth, J. Vander Auwera, P. Varanasi, K. Yoshino, J. Quantum Spectrosc. Radiat. Transf. **82**, 5 (2003)
10 M.T. McCulloch, E.L. Normand, N. Langford, G. Duxbury, D.A. Newnham, J. Opt. Soc. Am. B **20**, 1761 (2003)
11 C.R. Webster, G.J. Flesch, D.C. Scott, J.E. Swanson, R.D. May, W.S. Woodward, C. Gmachl, F. Capasso, D.L. Sivko, J.N. Baillargeon, A.L. Hutchinson, A.Y. Cho, Appl. Opt. **40**, 321 (2001)
12 J. Houghton, *The Physics of Atmospheres* (Cambridge University Press, Cambridge, UK, 2002), 3rd edn.
13 G. Duxbury, N. Langford, M.T. McCulloch, S. Wright, Mol. Phys. **105**, 741 (2007)
14 R.H. Dicke, Phys. Rev. **89**, 472 (1953)